Carbohydrate Research 346 (2011) 2785–2791

Contents lists available at SciVerse ScienceDirect

Carbohydrate Research

journal homepage: www.elsevier.com/locate/carres

Catalytic dehydration of xylose to furfural: vanadyl pyrophosphate as source of active soluble species

Irantzu Sádaba [a], Sérgio Lima [b], Anabela A. Valente [b,*], Manuel López Granados [a,*]

[a] *Institute of Catalysis and Petrochemsitry (CSIC), C/Marie Curie 2, Campus de Cantoblanco, 28049 Madrid, Spain*
[b] *Department of Chemistry, CICECO, University of Aveiro, Campus de Santiago, 3810-193 Aveiro, Portugal*

ARTICLE INFO

Article history:
Received 21 June 2011
Received in revised form 29 September 2011
Accepted 3 October 2011
Available online 8 October 2011

Keywords:
Xylose
Furfural
Acid catalysis
Vanadyl pyrophosphate
Homogeneous catalysis

ABSTRACT

The acid-catalysed, aqueous phase dehydration of xylose (a monosaccharide obtainable from hemicelluloses, e.g., xylan) to furfural was investigated using vanadium phosphates (VPO) as catalysts: the precursors, $VOPO_4{\cdot}2H_2O$, $VOHPO_4{\cdot}0.5H_2O$ and $VO(H_2PO_4)_2$, and the materials prepared by calcination of these precursors, that is, γ-$VOPO_4$, $(VO)_2P_2O_7$ and $VO(PO_3)_2$, respectively. The VPO precursors were completely soluble in the reaction medium. In contrast, the orthorhombic vanadyl pyrophosphate $(VO)_2P_2O_7$, prepared by calcination of $VOHPO_4{\cdot}0.5H_2O$ at 550 °C/2 h, could be recycled by simply separating the solid acid from the reaction mixture by centrifugation, and no drop in catalytic activity and furfural yields was observed in consecutive 4 h-batch runs (ca. 53% furfural yield, at 170 °C). However, detailed catalytic/characterisation studies revealed that the vanadyl pyrophosphate acts as a source of active water-soluble species in this reaction. For a concentration of $(VO)_2P_2O_7$ as low as 5 mM, the catalytic reaction of xylose (ca. 0.67 M xylose in water, and toluene as solvent for the in situ extraction of furfural) gave ca. 56% furfural yield, at 170 °C/6 h reaction.

1. Introduction

The depletion of fossil resources is promoting the search of alternative sources of energy and chemicals. Lignocellulose is appearing as a very attractive raw material, because it is abundant and inexpensive. In the context of the lignocellulosic-based biorefineries, furfural is acquiring increasing importance as one of the most outstanding building blocks.[1] It is one of the compounds in the 'top 10+4' revised list of bio-based product opportunities from carbohydrates.[2] Furfural is obtained via dehydration of xylose, which in turn is obtained from the hemicelluloses (polysaccharides) component of plant biomass (Scheme 1).[3] This reaction is industrially carried out in water as solvent, using liquid acids as catalysts such as, sulfuric acid which causes corrosion hazards, the formation of sulfur containing by-product, and enhanced waste production (e.g. from neutralisation processes). The development of less hazardous, 'greener' catalysts to perform this reaction in water is thus of important relevance to avoid the above mentioned drawbacks.

Several solid acids have been investigated as catalysts in the batchwise conversion of xylose into furfural such as, microporous zeolites and related materials,[4–7] micro-mesoporous silica-supported acids,[8–10] Keggin-type heteropolyacids,[11] titanates and niobates[12] and metal oxides.[13] These catalysts are solids and may therefore be easier and safer to handle in relation to liquid acids. Carlini et al. reported very interesting results for vanadium phosphate oxides (hereinafter referred to as VPO) used as acid catalysts in a similar reaction, that is, the dehydration of fructose to 5-hydroxymethyl-furfural (HMF),[14] using solely water as solvent, under relatively moderate reaction conditions. Recently, Wang et al. used different types of VPO acid catalysts in the dehydration of glycerol to acrolein.[15,16] To the best of our knowledge, VPO catalysts have not been investigated in the dehydration of xylose to furfural.

The crystalline structure and the surface morphology of VPO materials are dependent upon the preparation method of the precursor and the conditions of the calcination treatment (time, temperature, atmosphere).[16–19] Among the precursors the most common phases are those with a P/V atomic ratio of 1, namely, vanadyl phosphate dihydrate ($VOPO_4{\cdot}2H_2O$) and vanadyl hydrogen phosphate hemihydrate ($VOHPO_4{\cdot}0.5H_2O$). When $VOHPO_4{\cdot}0.5H_2O$ is calcined it may undergo a topotactic dehydration to form the vanadyl pyrophosphate $(VO)_2P_2O_7$, which is the typical industrial catalyst for the production of maleic anhydride from *n*-butane.[17] The thermal treatment of $VOPO_4{\cdot}2H_2O$ leads to different anhydrous phases like α_I-$VOPO_4$, α_{II}-$VOPO_4$, β-$VOPO_4$ and γ-$VOPO_4$ among others.[17] These materials have been widely studied as redox catalysts,[20,21] and to a much smaller extent as acid catalysts, even though VPO solids are known to possess acid properties.[19,22] Kamiya et al. reported that the pyrophosphate phase presents both Brønsted

---

* Corresponding authors. Tel.: +351 234370603; fax: +351 234401470 (A.A.V.); tel.: +34 915854937; fax: +34 915854760 (M.L.G.).

E-mail addresses: atav@ua.pt (A.A. Valente), mlgranados@icp.csic.es (M. López Granados).

0008-6215/$ - see front matter © 2011 Elsevier Ltd. All rights reserved.
doi:10.1016/j.carres.2011.10.001

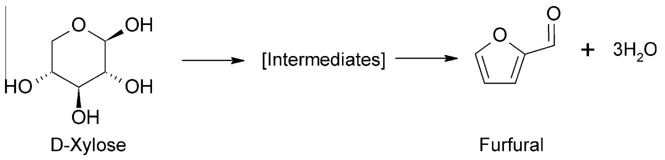

Scheme 1. Simplified reaction scheme of the dehydration of xylose to furfural.

and Lewis sites, and the acidic properties depended on the adopted preparation method.[23]

In the present work, the dehydration of D-xylose to furfural is investigated in the presence of vanadium phosphates as catalysts: $VOPO_4{\cdot}2H_2O$, $VOHPO_4{\cdot}0.5H_2O$ and $VO(H_2PO_4)_2$, and of the materials obtained by calcination of these precursors, γ-$VOPO_4$, $(VO)_2P_2O_7$ and $VO(PO_3)_2$, respectively. Special attention has been drawn to the assessment of the homo/heterogeneous catalytic contributions for the overall reaction of xylose; this issue was not previously addressed for VPO catalysts used in the dehydration of fructose to HMF.[14] Detailed characterisation and catalytic studies were carried out for the orthorhombic vanadyl pyrophosphate $(VO)_2P_2O_7$, prepared by calcination of $VOHPO_4{\cdot}0.5H_2O$ at 550 °C (most promising catalyst, based on catalytic screening tests).

2. Experimental

2.1. Catalyst preparation

Vanadyl phosphate dihydrate ($VOPO_4{\cdot}2H_2O$, denoted VP1-p) was synthesised in water according to the procedure described by Johnson et al.[24] Vanadium (V) pentoxide, V_2O_5 (5.0 g, 99.6% from Aldrich) was mixed with aqueous 85% *ortho*-phosphoric acid (30.0 mL, from Sigma-Aldrich) and deionised H_2O (120 mL). The mixture was refluxed while stirring for 24 h and a homogeneous yellow precipitate was obtained. The resulting precipitate was separated by filtration, and washed with hot distilled water (100 mL) and acetone (100 mL).[25] The solid was dried at 110 °C in an oven overnight, obtaining a greenish yellow powder.

Vanadyl hydrogen phosphate hemihydrate ($VOHPO_4{\cdot}0.5H_2O$, denoted VP2-p) was prepared by suspending V_2O_5 (15 g) in 90 mL of isobutyl alcohol (99%, Sigma-Aldrich) and 60 mL of benzyl alcohol (99%, Sigma-Aldrich). The suspension was stirred continuously under reflux for 3 h, cooled to room temperature, followed by the additions of *o*-H_3PO_4 (16.2 g, 99% from Sigma-Aldrich). The slurry was heated under reflux with constant stirring for 2 h, and subsequently cooled, filtered, washed with isobutyl alcohol and dried at 110 °C overnight to give a grey-blue powdered solid.[26]

The precursor $VO(H_2PO_4)_2$ (denoted VP3-p) was synthesised adapting the method proposed by Hannour et al.[27] V_2O_5 (18 g), H_3PO_4 (58 g) and water (400 ml) were mixed and heated in the presence of an excess of oxalic acid (10.1 g) at 90 °C for 48 h. The resulting blue solution was placed in a crystallizer and evaporated overnight. The resultant powdered solid was washed with acetone and dried.

Different calcination procedures were applied to the VP1-p, VP2-p and VP3-p precursors. The calcinations were conducted under static air in a muffle furnace or in N_2 flow using a Pyrex glass tube (internal diameter of 20 mm). The calcination conditions are summarised in Table 1. Following a procedure described by Zhu et al.,[22] VP1-c was prepared by calcination of $VOPO_4{\cdot}2H_2O$ (VP1-p), at 750 °C for 16 h, under air atmosphere to fully dehydrate the precursor. With the aim of preparing vanadyl pyrophosphate ($(VO)_2P_2O_7$), 0.5 g of VP2-p powdered solid was heated at 550 °C (10 °C min^{-1}) in N_2 flow (60 mL min^{-1}) during 2 h (giving a solid denoted VP2-550-2h).[28] Since VP2-550-2h gave promising catalytic results (discussed ahead), the influence of the calcination temperature and time applied to the VP2-p precursor, was investigated. These samples are denoted as VP2-X-Yh, where X refers to the calcination temperature (°C) and Y to the calcination time (h). $VO(H_2PO_4)_2$ (VP3-p) was calcined at 500 °C in N_2 flow (same conditions as for VP2) during 16 h to obtain a solid denoted VP3-c ($VO(PO_3)_2$).[29]

2.2. Catalyst characterisation

Powder XRD data were collected at room temperature on a Philips X'pert Pro PANalytical diffractometer with Cu-Kα_1 (λ = 0.154046 nm) and Cu-Kα2 (λ = 0.154443 nm) radiations (Kα1/Kα2 = 0.5), in a Bragg–Brentano para-focusing optics configuration (40 kV, 50 mA). Samples were step-scanned in 0.02° steps with a counting time of 50 s per step. Diffractograms were analysed with the X'Pert HighScore Plus software. N_2 adsorption–desorption isotherms were recorded at −196 °C using a Micromeritics TRISTAR 3000 apparatus; the samples were degassed at 120 °C for 12 h prior analysis. Thermogravimetric (TGA) and differential scanning calorimetry (DSC) analyses were performed with Shimadzu TGA-50 and DSC-50 systems (heating rate of 10 °C min^{-1} under air), respectively. An inductively coupled plasma mass spectrometer (ICP-MS) Elan 6000 Perkin-Elmer Sciex equipped with an AS 91 autosampler, was used for quantification of V and P.

Diffuse Reflectance Infrared Fourier Transform Spectroscopy (DRIFTS) of the NH_3 adsorption was carried out to evaluate the acid properties of the solids. Spectra were collected on a Nicolet 5700 FT spectrophotometer equipped with a high sensitivity Hg–Cd–Te detector and a Praying Mantis (Harrick Scientific Co.) optical accessory to focus the IR beam on the sample. A high temperature in situ chamber (Harrick Scientific Co.) with Zn Se windows was used for thermal treatment of the samples before recording the DRIFT spectra. Spectra were obtained at a resolution of 4 cm^{-1} with an accumulation of 256 scans and presented in Kubelka-Munk mode. Typically, the finely ground samples (ca. 50 mg) were placed in the cup of the in situ DRIFT chamber. The calcined sample was pretreated under Ar flow (ca. 50 mL min^{-1}, Air Liquide) at 150 °C for 60 min and cooled down at 30 °C. Then, NH_3 (50 mL min^{-1}, 900 ppm in Ar, Air Liquide) was passed through the sample for 30 min at that temperature. The sample was subsequently evacuated under Ar flow for 30 min at 30, 100, 200, 300 and 400 °C before recording the IR spectra. For each temperature, the spectra of the sample without exposure to NH_3 were recorded and subtracted from the spectrum of the same sample exposed to NH_3.

2.3. Catalytic reactions

Batch catalytic experiments were performed in glass micro-reactors equipped with magnetic stirring bars. The micro-reactors were always purged with nitrogen prior to heating. In a typical procedure, 30 mg of D-xylose (SigmaUltra, >99%), 20 mg of catalyst and H_2O (0.3 mL, Milli-Q) and toluene (0.7 mL, Chromasolv Plus, >99.9%) were poured into the reactor. The reaction mixture was heated with a thermostatically controlled oil bath and stirred magnetically at 800 rpm. Zero time was taken when the micro-reactor was immersed in the oil bath. In the catalyst recycling tests, the solid was separated from the reaction mixture by centrifugation at the selected times, washed and sonicated for 5 min in water, methanol and acetone, dried at 50 °C overnight (denoted W-treatment). For comparison, the washed solid was subsequently calcined at 400 °C (heating rate of 10 °C min^{-1}, static air) for 2 h (denoted WC-treatment). The analysis of D-xylose and furfural in the aqueous phase was quantitatively determined using an HPLC equipped with a Knauer K-1001 HPLC pump and a PL Hi-Plex H 300 × 7.7 (i.d.) mm ion-exchange column (Polymer Laboratories Ltd., UK) coupled to a Knauer K-2401 differential refractive index

Table 1
Synthetic conditions and physical properties of the prepared VPO solids

Sample	Crystalline Phase	Synthetic precursor/calcination conditions	Colour	S_{BET}[a] ($m^2\ g^{-1}$)
VP1-p	$VOPO_4{\cdot}2H_2O$[b]	–	Green	0.3
VP2-p	$VOHPO_4{\cdot}0.5H_2O$	–	Blue-grey	36.2
VP3-p	$VO(H_2PO_4)_2$	–	Turquoise	0.2
VP1-c	γ-$VOPO_4$	VP1/750 °C, 16 h, air	Yellow	5.1
VP2-550-2h	$(VO)_2P_2O_7$[c]	VP2/550 °C, 2 h, N_2	Dark brown	37.2
VP3-c	$VO(PO_3)_2$[d]	VP3/500 °C, 16 h, N_2	Turquoise	Nm[e]

[a] Brunauer–Emmett–Teller (BET) specific surface area.
[b] Contains $(VO)(VO_2)_2H_4(PO_4)_2(P_2O_7)_{0.5}{\cdot}H_2O$.
[c] Contains $VO(H_2PO_4)_2$ impurity.
[d] Contains $V(PO_3)_3$ impurity.
[e] Not measurable.

detector (for xylose) and a Knauer K-2600 UV detector (280 nm, for furfural). The mobile phase was water acidified to pH 3.05 with H_2SO_4. The flow rate was 0.6 mL min^{-1} and the column temperature was maintained at 65 °C. The furfural present in the organic phase was quantified with a Gilson 306 HPLC pump and a Spherisorb ODS S10 C18 column, coupled to a Gilson 118 UV/Vis detector (280 nm). The mobile phase consisted of 40% v/v methanol in water (flow rate 0.7 mL min^{-1}).

3. Results and discussion

3.1. Characterisation and screening catalytic tests of the VPO precursors

The colours of the VPO precursors (VP1-p, VP2-p and VP3-p) are given in Table 1, and are indicative of the oxidation state of the vanadium (blue and yellow is characteristic of V^{4+} and V^{5+} ions, respectively). The powder XRD pattern of VP1-p shows a well-crystallised dihydrate phase $VOPO_4{\cdot}2H_2O$ (1, PDF Reference code 01-084-0111) containing $(VO)(VO_2)_2H_4(PO_4)_2(P_2O_7)_{0.5}{\cdot}H_2O$ (PDF Reference code 00-047-0967) as an impurity (Fig. 1). The VP2-p solid consists of the hemihydrate phase $VOPO_4{\cdot}2H_2O$ (2, PDF Reference code 00-038-0291), and the VP3-p pattern is assigned to the tetragonal $VO(H_2PO_4)_2$ phase (3, PDF Reference code 00-047-0953). In general, the BET specific surface areas of the samples are quite low, and the highest value was obtained for VP2-p (36 $m^2\ g^{-1}$), which parallels that observed for the respective calcined solids (discussed ahead), Table 1; these results are in agreement with the literature data.[20,23,30]

The reaction of xylose was investigated using the VPO precursors as catalysts, which were completely soluble in the reaction medium. Carlini and co-workers reported interesting results when using modified vanadyl phosphate dihydrate ($VOPO_4{\cdot}2H_2O$) as catalyst in the dehydration of fructose to HMF, at 80 °C, using solely water as solvent[14]: 79% HMF selectivity at 50% conversion within 1 h of reaction. Under these conditions, the reaction of xylose in the presence of VP1-p ($VOPO_4{\cdot}2H_2O$) does not take place. Possibly, more demanding acid conditions are required for the dehydration of xylose (aldose, pentose) than those for fructose (ketose, hexose). The reaction of xylose in the presence of VP2-p, at 170 °C, using a biphasic water–toluene solvent system, (which is favourable for enhancing furfural selectivity, as discussed ahead), is quite fast giving 100% conversion in less than 2 h reaction, albeit the selectivity towards furfural being always less than 50%. The VP3-p precursor was poorly active in this reaction.

3.2. Characterisation and screening catalytic tests of the calcined solids

The calcination of the VPO precursors (VP1-p, VP2-p and VP3-p) under appropriate conditions gave the solids VP1-c, VP2-550-2h and VP3-c, respectively. According to the powder XRD data, the VP1-c solid consists of a monoclinic γ-$VOPO_4$ phase, according to Bordes[17] (1, PDF Reference code 00-047-0950), Figure 2. Although the applied calcination treatment was similar to that reported previously by Zhu et al.[22] to obtain tetragonal α_{II}-$VOPO_4$, the latter phase was not detected in the case of VP1-c. The VP2-550-2h solid consists of an orthorhombic phase of vanadyl pyrophosphate

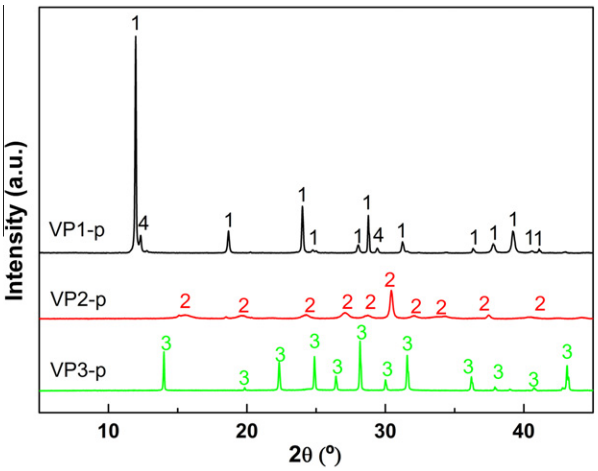

Figure 1. Powder X-ray diffraction patterns of the precursors. The data labels correspond to the following crystalline phases: **1**—$VOPO_4{\cdot}2H_2O$, **2**—$VOHPO_4{\cdot}0.5H_2O$, **3**—$VO(H_2PO_4)_2$, **4**—$(VO)(VO_2)_2H_4(PO_4)_2(P_2O_7)0.5{\cdot}H_2O$.

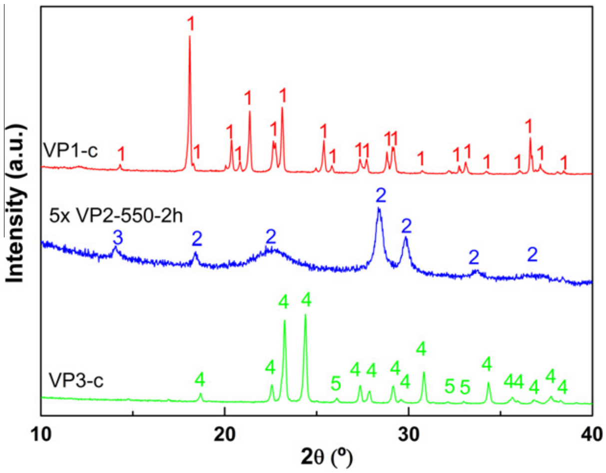

Figure 2. Powder X-ray diffraction patterns of the calcined solids. The data labels correspond to the following crystalline phases: **1**—γ-$VOPO_4$, **2**—$(VO)_2P_2O_7$, **3**—$VO(H_2PO_4)_2$, **4**—$VO(PO_3)_2$, **5**—$V(PO_3)_3$.

$(VO)_2P_2O_7$ (2, PDF Reference code 00-041-0698) containing $VO(H_2PO_4)_2$ as a minor impurity (3, PDF Reference code 00-047-0953). The XRD pattern of this solid matches that reported by other authors using the same calcination conditions.[16] The calcination of VP3-p produced a well crystallised $VO(PO_3)_2$ phase (4, PDF Reference code 00-033-1433), containing $V(PO_3)_3$ as a minor impurity (5, PDF Reference code 00-033-1442). In general, the BET specific surface areas of the samples are quite low, and the highest value was obtained for VP2-550-2h (ca. 37 $m^2\,g^{-1}$), which is similar to that observed for its precursor VP2-p (Table 1).

Based on preliminary catalytic tests of the investigated materials (discussed ahead), the VP-2, which was apparently insoluble in the reaction medium, seemed a quite promising catalyst. Hence, the effect of the calcination conditions on the crystalline structure and the surface acid properties of VP-2 were further investigated. The calcination time and temperature of VP2-p caused structural modifications. The colours of the VP2-550-Yh samples are different: dark brown, grey and greenish for calcination time of 2, 8 and 16 h, respectively. For longer calcination time (16 h) new reflections appeared at ca. 15° 2θ, assigned to the monoclinic phase of vanadyl pyrophosphate (2, PDF Reference code 01-085-2281), Figure 3. In general, these solids are nanocrystalline and the crystallite size tends to increase slightly with increasing calcination time at 550 °C (Table 2); concomitant narrowing of the peaks at $2\theta = 22.6°$ and 28.2° is observed. Apparently the crystallinity increases faster on the perpendicular direction of the (020) planes. Calcination at a higher temperature of 750 °C (N_2 atmosphere) resulted in a less crystalline orthorhombic $(VO)_2P_2O_7$ phase and a new phase appeared as orthorhombic VPO_4, indicating the partial reduction of vanadium, under these conditions.

The effect of the calcination treatment on the acid properties of the VP2-derived catalysts was investigated by DRIFT analysis of NH_3 adsorbed on Lewis (LAS) and Brønsted (BAS) acid sites (bands appearing in the region 2000–1200 cm^{-1}). The NH_3 molecule chemisorbed on LAS displays a δ_{as} (H–N–H) band at ca. 1650 cm^{-1}, whereas NH_4^+ formed over BAS shows another band at ca. 1425 cm^{-1}, due to δ_{as} (H–N–H).[31–34] According to the literature, the ratio of the absorption coefficients of the bands 1425 and 1650 cm^{-1} (NH_4^+/NH_3) is close to 7, which means that the band assigned to LAS is usually much weaker.[35] Busca et al.[36] assigned the BAS to surface P–OH groups and the LAS to coordinatively unsaturated V(IV) ions exposed on the surface. Figure 4 shows the δ_{as} (H–N–H) bands of NH_3 and NH_4^+ adsorbed on the catalysts VP2-550-2h and VP2-750-2h, after different outgassing temperatures. The most intense band was the one at 1425 cm^{-1} indicating that in these catalysts BAS predominate over LAS. The band assigned to the asymmetric deformation modes of chemisorbed NH_3 at ca. 1650 cm^{-1} was vaguely detected in the case of the VP2-550-2h. Possibly, the activation temperature used in this experiment (150 °C) was not high enough to completely remove the chemisorbed water and form the LAS. Negative bands in the 3600–3500 cm^{-1} region (not shown) were due to the disappearance of the surface hydroxyl groups.

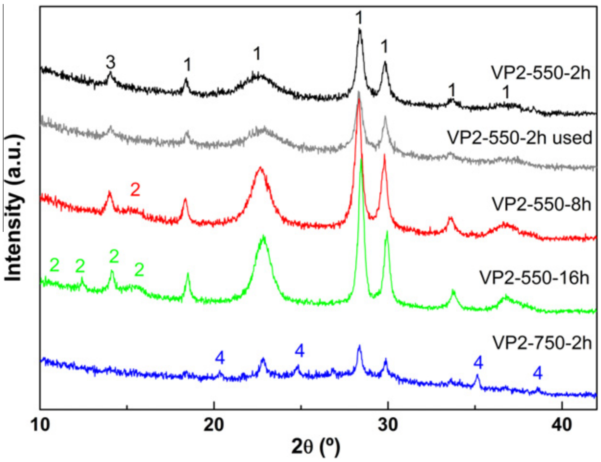

Figure 3. Powder XRD patterns of the vanadyl pyrophosphate materials prepared using different calcination temperatures and times and of VP2-550-2h after the catalytic reaction (VP2-550-2h used). **1**—orthorhombic $(VO)_2P_2O_7$, **2**—monoclinic $(VO)_2P_2O_7$, **3**—$VO(H_2PO_4)_2$, **4**—VPO_4.

Table 2
Crystallite sizes of the calcined solids

Catalyst	Crystallite size[a] (nm)	
	020[b]	204[c]
VP2-550-2h	4.5	16.7
VP2-550-2h-used	4.9	16.2
VP2-550-8h	6.9	17.5
VP2-550-16h	8.2	21.7
VP2-750-2h	11.6	19.5

[a] Calculated by the Debye–Scherrer equation.
[b] Crystallite sizes calculated using the full width at half-maximum of (020) reflection at ca. 22.6°.
[c] Crystallite sizes calculated using the full width at half-maximum of (204) reflection at ca. 28.2°.

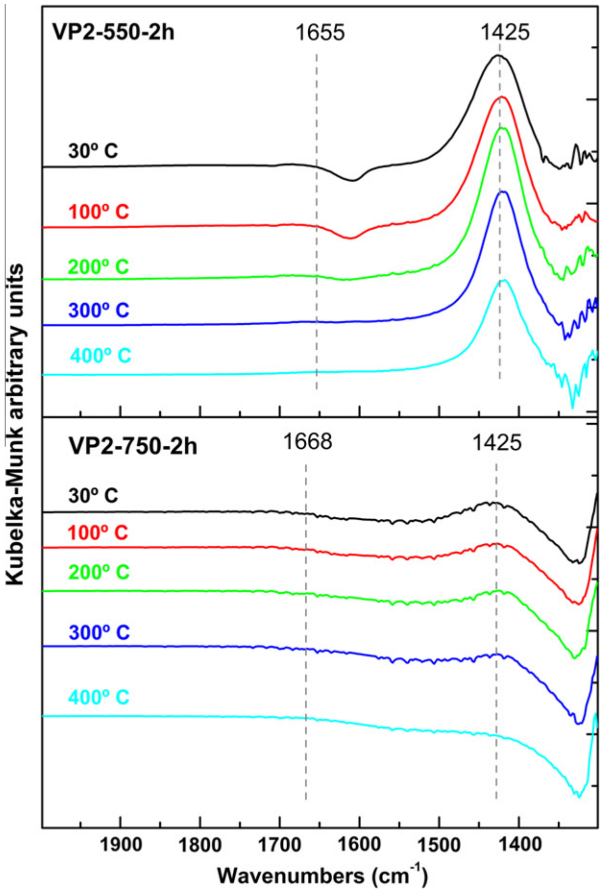

Figure 4. DRIFT spectra of the NH_3 adsorption over (top) VP2-550-2h and (bottom) VP2-750-2h for the indicated outgassing temperatures.

The band assigned to BAS becomes weaker with increasing outgassing temperature (Fig. 4). In the case of VP2-550-2h, the presence of a strong band at 1425 cm^{-1} even after evacuation at 400 °C, which was not observed for VP2-750-2h, indicates that the BAS of VP2-

Table 3
Integrated area (IA) of the infrared band at 1425 cm^{-1} (assigned to BAS, Kubelka-Munk arbitrary units) as a function of the outgassing temperature of the VP2-X-Yh solids

Temperature (°C)	VP2-550-2h	VP2-550-16h	VP2-750-2h
30	1499	1376	989
100	1044	1170	715
200	675	590	271
300	539	585	252
400	519	437	–

550-2h are stronger. Table 3 shows the integrated areas (IAs) of the band at 1425 cm^{-1} for the spectra given in Figure 4, and for the VP2-550-16h sample. The IAs of the bands of VP2-550-2h and VP2-550-16h samples were quite similar for all outgassing temperatures, suggesting that calcination time at 550 °C does not affect significantly the acid properties. The VP2-750-2h sample possesses a lower amount of acid sites (based on the lower values of IAs) than the VP2-550-Xh solids, which can be related to the comparatively lower crystallinity of this sample and/or to the presence of the VPO_4 impurity phase (Fig. 3).

The catalytic performance of the calcined solids was investigated preliminarily using solely water as solvent, at 170 °C (Table 4, entries 1, 4 and 6). For all materials, excluding VP3-c, the conversion of xylose at 4 h reaction is quite high (70–80%), but the furfural yields are rather low (<25%). The liquid phase obtained after the catalytic tests was coloured for the VP1-c (colour changed instantly) and VP3-c solids, indicating the dissolution of metal species. The same was not observed for VP2-c, which gave the highest furfural yield. Hence, the reaction of xylose was further investigated in the presence of VP2-c.

3.3. Reaction of xylose in the presence of VP2-X-Yh solid acids

In the case of VP2-550-2h as catalyst, decreasing the temperature of the reaction of xylose from 170 to 140 °C leads to a considerable decrease in the conversion and the furfural yield, which are even lower at 120 °C (Table 4, entries 2–4). The mechanism of the dehydration of xylose may take place as an acid-catalysed series of elementary steps proceeding through a 2,5-anhydride intermediate.[37] In the present work, by-products were not detected by HPLC analysis. However, according to the literature, furfural can further react with itself, 'furfural resinification', or with intermediates of the pentose-to-furfural conversion, 'furfural condensation', leading to higher molecular weight products.[3] On the other hand, fragmentation reactions of xylose can take place in parallel to furfural formation.[37]

In order to improve the selectivity to furfural, toluene was used as a co-solvent (forming a biphasic solvent system) for extracting furfural from the aqueous phase. Since the catalysts' surface is polar (e.g. possess surface P–OH groups), the solid particles dispersed preferably in the aqueous phase. Once furfural is formed and transferred into the organic phase one may expect that its adsorption on the polar surface of the catalyst becomes less favourable than without the organic co-solvent, avoiding its degradation by acid species. A comparison of the results in Table 4 (entries 4 and 5) for the reaction of xylose at 170 °C in the presence of VP2-550-2h shows the beneficial effect of using toluene as a co-solvent on furfural yield at 4 h (ca. two-fold increase).

The effect of calcination time and temperature on the catalytic performance of VP2-p was investigated in the reaction of xylose at 170 °C, under biphasic solvent conditions. In all the cases, at least 90% conversion was reached within 6 h of reaction (Fig. 5). The precursor VP2-p was much more active than the VP2-X-Yh counterparts (Fig. 5a), but the selectivity to furfural was much lower (Fig. 5b). The kinetic profiles and the curves of the dependency of furfural selectivity on conversion are fairly coincident for all the VP2-550-Xh samples, indicating that the influence calcination time on the catalytic performance was not significant. In principle, these results seem to correlate very well with the similar acid properties of these catalysts (Table 3). In comparison to VP2-550-2h, the VP2-750-2h sample possesses lower catalytic activity (60% compared to 75% conversion at 2 h for VP2-550-2h, respectively, Fig. 5a). Despite the higher reaction times required to reach ca. 90% conversion in the case of VP2-750-2 h, somewhat higher furfural selectivity was reached (Fig. 5b). These results may be due to the weaker acidity of this latter sample. It is interesting to stress that furfural selectivity increases with conversion possibly because the primary step of conversion of xylose is faster than one of the subsequent steps, leading to relatively slow increase in concentration of furfural in the bulk (Fig. 5b).[6]

The stability of the VP2-550-2h catalyst was investigated by performing consecutive 4 h-batch runs for the reaction of xylose at 170 °C, under biphasic solvent conditions. Prior to catalyst recycling, the solid was separated from the reaction medium by centrifugation, followed by a washing treatment (denoted W-treatment) or washing plus calcination treatment (denoted WC-treatment); experimental details are given in Section 2.3. The conversions of xylose were somewhat comparable in the three consecutive runs (90%, 80% and 86% for runs 1, 2 and 3, respectively). Figure 6 shows that furfural yields in the first couple of runs are comparable for the two catalyst treatments and remains fairly constant in the third run by simply using the W-treatment. These results contrast with those reported in the literature for some families of solid acid catalysts investigated in the reaction of xylose, which required thermal treatments for the recovery of the initial catalytic performance.[6–8,10,38] These contrasting results may be due to differences in the homo/heterogeneous nature of the catalytic reaction (discussed ahead).

The powder XRD patterns of the fresh and washed catalysts (Fig. 3) were quite similar and the crystallite sizes are comparable (Table 2), suggesting that the structure of the solid can be relatively stable under the applied hydrothermal conditions. Elemental analysis revealed that the VP2-550-2h solid recovered by the W-treatment contained 7 wt % of carbon. A comparative study of the TGA and DSC analyses (Fig. 7) for the fresh and used catalysts shows that the used catalyst undergoes a different exothermic process in the temperature range 250–400 °C, which may be related to

Table 4
Catalytic results for the calcined VPO catalysts[a]

Entry	Sample	Temperature (°C)	Xylose conversion (%)	Furfural yield (%)	Furfural selectivity (%)
1	VP1-c	170	71	22	31
2	VP2-550-2h	120	21	7	33
3	VP2-550-2h	140	33	8	23
4	VP2-550-2h	170	80	24	29
5	VP2-550-2h[b]	170	91	53	58
6	VP3-c	170	13.4	3.8	28

[a] Reaction conditions: 30 mg of xylose, substrate/catalyst mass ratio = 1.5, 1 mL H_2O, 4 h.
[b] 1 mL water–toluene solvent mixture (3:7 volume ratio).

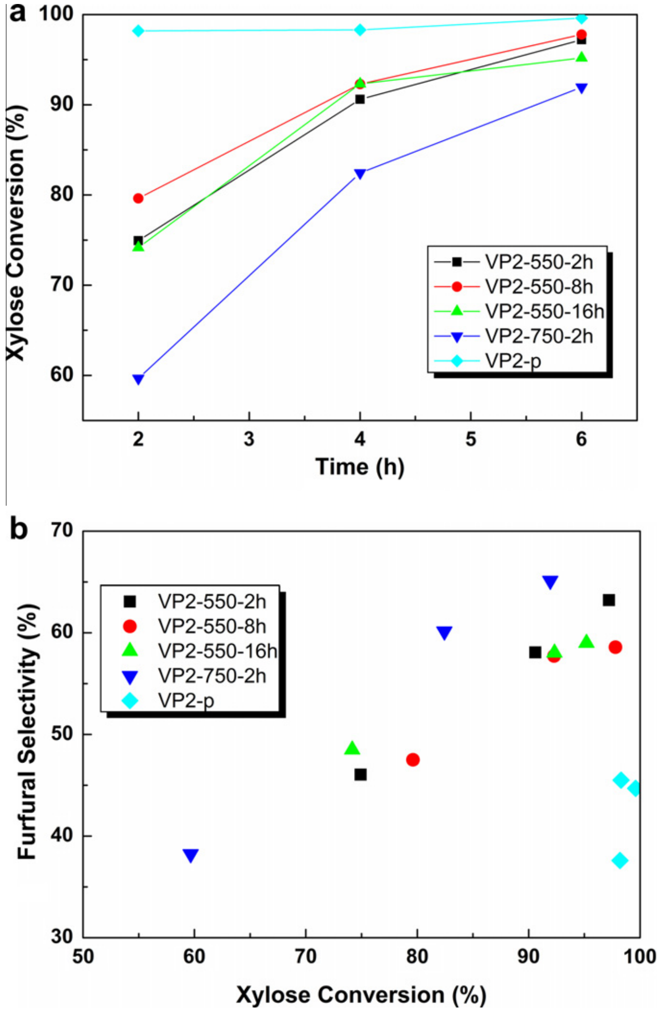

Figure 5. Kinetic profiles of the xylose conversion (a) and dependence of furfural selectivity on xylose conversion (b), for the VP2-p precursor and the respective calcined catalysts. Reaction conditions: 30 mg of xylose, substrate/catalyst mass ratio = 1.5, 170 °C, 1 mL water–toluene mixture (3:7 volume ratio).

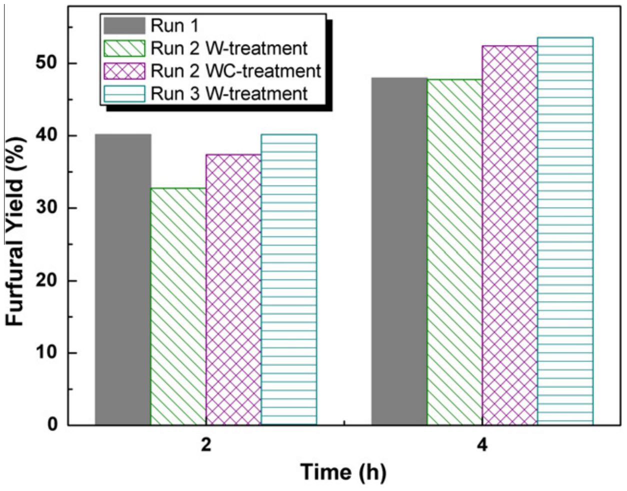

Figure 6. Furfural yields in consecutive 4 h-batch runs, at 170 °C, using VP2-550-2h as catalyst, and applying the W-treatment (runs 2 and 3 washed) or the WC-treatment (run 2 calcined) to the separated solid prior to its reuse. Reaction conditions as in Figure 5.

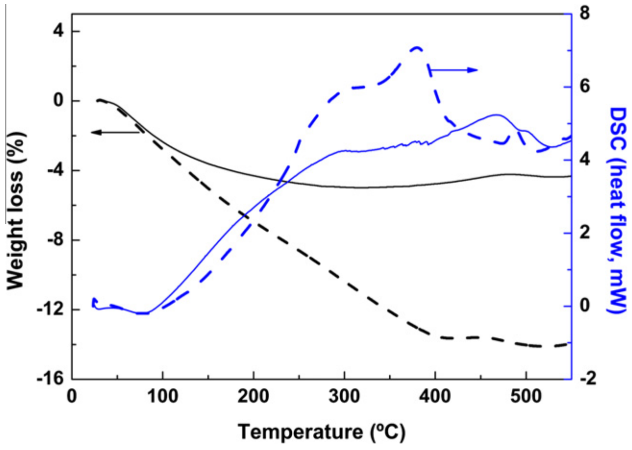

Figure 7. TGA and DSC curves of fresh (solid line) and used (dashes) VP2-550-2h catalyst. Reaction conditions as in Figure 5.

the combustion of organic matter (a small endothermic band below 120 °C is associated to the desorption of physisorbed water/volatiles). Comparing the mass losses between the fresh and used catalysts, one may deduce that the amount of organic matter is ca. 9 wt % of the VP2-550-2h solid, which is consistent with the elemental analysis result. The amount of organic matter in the recovered solid is significantly lower than that reported in the literature for other solid acids tested as catalysts in the same reaction, under similar conditions in which xylose conversion reached at least 90%.[7] Apparently, the hydrothermal stability of the $(VO)_2P_2O_7$ phase and the small amount of organic deposits would explain the steadiness of the catalytic properties in recycling runs. However ICP-MS analyses of the aqueous phase after the reaction showed that the V and P concentrations in the solution after the first run were 527 and 320 ppm respectively. These are minor amounts and are equivalent to ca. 5 mmol$_{(VO)_2P_2O_7}$/L, or ca. 2.3 mol % of the initial catalyst loading of 217 mmol$_{(VO)_2P_2O_7}$/L (under typical reaction conditions).

In order to get insight on the homogeneous contribution of the solubilised species, a separate experiment was performed in which the catalyst was put into contact with water (without xylose) at 170 °C, during 4 h; subsequently the reaction mixture was cooled to room temperature, the solid acid was filtered through a 0.2 μm PVDF w/GMF Whatman membrane, and xylose and toluene were added to the resulting aqueous phase, which was then heated to 170 °C. After 4 h reaction, the xylose conversion and furfural yield were similar to those observed for the catalytic test using 20 mg of solid catalyst, indicating the existence of a homogeneous catalytic contribution. In order to assess the extent of the homogeneous catalytic contribution, a separate catalytic test was carried out using VP2-550-2h in an amount equivalent to that measured by ICP-MS (5 mM $(VO)_2P_2O_7$): the conversion and furfural yields at 2 h/6 h reaction were similar (differences within the experimental range of order of ca. 10%) to those observed for the catalytic reaction using 20 mg of VP2-550-2h catalyst (equivalent to 217 mM $(VO)_2P_2O_7$ in the aqueous phase). These results suggest that the catalytic reaction takes place essentially in the homogeneous phase and that the VP2-550-2h solid acts as a supplier of very active soluble species. These results can partly explain (i) the 'steady' catalytic performance of VP2-550-2h in consecutive batch runs since an excess amount of catalyst was used (Fig. 6), and (ii) the fact that the type of treatment (W or WC) applied to the separated solid acid, on the catalytic reaction of xylose, was minor.

For comparative purposes, the water-soluble salts $NaHPO_4$ (10 mM), $VOSO_4$ (10 mM), $Na_4P_2O_7$ (5 mM), and a mixture of $VOSO_4$ (10 mM) and $Na_4P_2O_7$ (5 mM) were tested as homogeneous

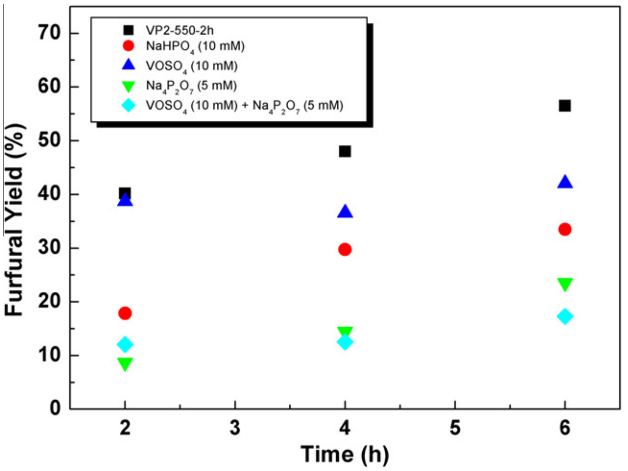

Figure 8. Furfural yield versus reaction time, using as catalysts the (soluble) salts, $NaHPO_4$ (10 mM), $VOSO_4$ (10 mM), $Na_4P_2O_7$ (5 mM) or a mixture of $VOSO_4$ (10 mM) and $Na_4P_2O_7$ (5 mM); the data for VP2-550-2h are given for comparison. Reaction conditions: 30 mg of xylose, 170 °C, 1 mL water–toluene mixture (3:7 volume ratio).

catalysts (used in amounts equivalent to the approximate leached amounts of V and P observed for VP2-550-2h), in the reaction of xylose, at 170 °C. The furfural yield reached at 6 h reaction follows the order, ($Na_4P_2O_7$+$VOSO_4$) (17%) < $Na_4P_2O_7$ (24%) < $NaHPO_4$ (34%) < $VOSO_4$ (42%) < VP2-550-2h (56%), Figure 8. Based on these results, the catalytic performance of the VP2-550-2h catalyst is different from those of the tested salts (containing similar ions), leading to higher furfural yields, under similar reaction conditions.

4. Conclusions

The dehydration of xylose can be effectively carried out in the presence of vanadium phosphates as catalysts. The $(VO)_2P_2O_7$ material (denoted VP2-550-2h), prepared by calcination of the precursor $VOHPO_4{\cdot}0.5H_2O$ at 550 °C/2 h, exhibited superior catalytic performance amongst the investigated materials. The VP2-550-2h solid was essentially insoluble in the reaction medium, and catalytic tests and solid state characterisation studies of the solid separated after the catalytic reaction, revealed that (i) the catalytic results correlated with the surface acid properties; (ii) the solid could be recycled without drop in catalytic activity and furfural yields (ca. 53% at 4 h reaction); (iii) no significant structural modifications of the recovered solid were observed. Based on these results, one could conclude that the catalytic reaction of xylose in the presence of VP2-550-2h is heterogeneous in nature. However, detailed studies based on ICP-MS analyses coupled with catalytic tests (directed towards the assessment of homo/heterogeneous nature of the catalytic reaction) indicated that the VP2-550-2h solid actually acts as a source of very active (present in minor amounts) water-soluble species, which are responsible for the observed catalytic activity. The VP2-550-2h catalyst leads to higher furfural yields than for the soluble salts (containing similar ions), $VOSO_4$ and $Na_4P_2O_7$ (or their mixture), under similar reaction conditions. A concentration of $(VO)_2P_2O_7$ as low as 5 mM, led to ca. 56% furfural yield, at 170 °C/6 h reaction. It is worth stressing the importance of conducting experiments in order to unveil the effective homo/heterogeneous nature of the catalytic reaction because soluble species can be extremely active, requiring minor amounts for performing effectively the catalytic reaction.

In overall, furfural can be effectively synthesised via the dehydration of xylose in the presence of minor amounts of $(VO)_2P_2O_7$ and, in this case, the catalyst recycling could involve the separation of the toluene phase from the aqueous one (decantation) after the reaction of xylose, the recovery of furfural by distillation, and the used toluene extracting solvent could be recharged to the reactor containing the aqueous phase with the soluble catalyst for initialising a subsequent run.

Acknowledgements

This work was partially funded by the Spanish Ministry of Science and Innovation (MICINN: ENE-2009-12743-C04-01), ‘Consejería de Educación’ of the Autonomous Government of Madrid (CAM: CARDENER-CM) and the Portuguese Fundação para a Ciência e a Tecnologia (FCT), POCI and FEDER (project POCI/QUI/56112/2004). I. Sádaba is grateful to the Spanish National Research Council (CSIC) for a JAE-Predoc and for the financial support for the stay at CICECO, University of Aveiro. S. Lima is grateful to the FCT for post-doctoral grant. The authors wish to express their gratitude to Dr. F. Domingues (Department of Chemistry, University of Aveiro) for access to HPLC equipment and to Doctor Martyn Pillinger (CICECO, University of Aveiro) for helpful discussions.

References

1. *Biorefineries—Industrial Processes and Products Status Quo and Future Directions*; Kamm, B., Gruber, P. R., Kamm, M., Eds.; Wiley-VCH: Weinheim, 2005.
2. Bozell, J. J.; Petersen, G. R. *Green Chem.* **2010**, *12*, 539–554.
3. Zeitsch, K. J. The Chemistry and Technology of Furfural and Its Many By-Products, 1st ed. In *Sugar Series*; Elsevier: The Netherlands, 2000; Vol. 13,.
4. Moreau, C.; Durand, R.; Peyron, D.; Duhamet, J.; Rivalier, P. *Ind. Crops Prod.* **1998**, *7*, 95–99.
5. O'Neill, R.; Ahmad, M.; Vanoye, L.; Aiouache, F. *Ind. Eng. Chem. Res.* **2009**, *48*, 4300–4306.
6. Lima, S.; Fernandes, A.; Antunes, M. M.; Pillinger, M.; Ribeiro, F.; Valente, A. A. *Catal. Lett.* **2010**, *135*, 41–47.
7. Lima, S.; Antunes, M. M.; Fernandes, A.; Pillinger, M.; Ribeiro, F.; Valente, A. A. *Appl. Catal., A* **2010**, *388*, 141–148.
8. Dias, A. S.; Pillinger, M.; Valente, A. A. *J. Catal.* **2005**, *229*, 414–423.
9. Dias, A. S.; Pillinger, M.; Valente, A. A. *Microporous Mesoporous Mater.* **2006**, *94*, 214–225.
10. Shi, X.; Wu, Y.; Li, P.; Yi, H.; Yang, M.; Wang, G. *Carbohydr. Res.* **2011**, *346*, 480–487.
11. Dias, A. S.; Pillinger, M.; Valente, A. A. *Appl. Catal., A* **2005**, *285*, 126–131.
12. Dias, A. S.; Lima, S.; Carriazo, D.; Rives, V.; Pillinger, M.; Valente, A. A. *J. Catal.* **2006**, *244*, 230–237.
13. Chareonlimkun, A.; Champreda, V.; Shotipruk, A.; Laosiripojana, N. *Bioresour. Technol.* **2010**, *101*, 4179–4186.
14. Carlini, C.; Patrono, P.; Galletti, A. M. R.; Sbrana, G. *Appl. Catal., A* **2004**, *275*, 111–118.
15. Wang, F.; Dubois, J.-L.; Ueda, W. *J. Catal.* **2009**, *268*, 260–267.
16. Wang, F.; Dubois, J.-L.; Ueda, W. *Appl. Catal., A* **2010**, *376*, 25–32.
17. Bordes, E. *Catal. Today* **1987**, *1*, 499–526.
18. Taufiq-Yap, Y. H.; Saw, C. S. *Catal. Today* **2008**, *131*, 285–291.
19. Landi, G.; Lisi, L.; Volta, J. C. *J. Mol. Catal. A: Chem.* **2004**, *222*, 175–181.
20. Hutchings, G. J. *J. Mater. Chem.* **2004**, *14*, 3385–3395.
21. Cavani, F.; De Santi, D.; Luciani, S.; Löfberg, A.; Bordes-Richard, E.; Cortelli, C.; Leanza, R. *Appl. Catal., A* **2010**, *376*, 66–75.
22. Zhu, Y. J.; Li, J.; Xie, X. F.; Yang, X. G.; Wu, Y. *J. Mol. Catal. A: Chem.* **2006**, *246*, 185–189.
23. Kamiya, Y. *J. Jpn. Pet. Inst.* **2003**, *46*, 62–68.
24. Johnson, J. W.; Johnston, D. C.; Jacobson, A. J.; Brody, J. F. *J. Am. Chem. Soc.* **1984**, *106*, 8123–8128.
25. Griesel, L.; Bartley, J. K.; Wells, R. P. K.; Hutchings, G. J. *J. Mol. Catal. A: Chem.* **2004**, *220*, 113–119.
26. Albonetti, S.; Cavani, F.; Trifirò, F.; Venturoli, P.; Calestani, G.; López Granados, M.; Fierro, J. L. G. *J. Catal.* **1996**, *160*, 52–64.
27. Hannour, F. K.; Martin, A.; Kubias, B.; Lücke, B.; Bordes, E.; Courtine, P. *Catal. Today* **1998**, *40*, 263–272.
28. Igarashi, H.; Tsuji, K.; Okuhara, T.; Misono, M. *J. Phys. Chem.* **1993**, *97*, 7065–7071.
29. Sananes, M. T.; Hutchings, G. J.; Volta, J. C. *J. Catal.* **1995**, *154*, 253–260.
30. Rownaghi, A. A.; Taufiq-Yap, Y. H.; Rezaei, F. *Ind. Eng. Chem. Res.* **2009**, *48*, 7517–7528.
31. Cornaglia, L. M.; Lombardo, E. A.; Andersen, J. A.; Fierro, J. L. G. *Appl. Catal., A* **1993**, *100*, 37–50.
32. Jung, S. M.; Grange, P. *Appl. Catal., B* **2002**, *36*, 325–332.
33. Centeno, M. A.; Carrizosa, I.; Odriozola, J. A. *J. Alloys Compd.* **2001**, *323–324*, 597–600.
34. Sun, D.; Liu, Q.; Liu, Z.; Gui, G.; Huang, Z. *Appl. Catal., B* **2009**, *92*, 462–467.
35. Van Tongelen, M. *J. Catal.* **1966**, *5*, 535–537.
36. Busca, G.; Centi, G.; Trifiró, F.; Lorenzelli, V. *J. Phys. Chem.* **1986**, *90*, 1337–1344.
37. Antal, M. J.; Leesomboon, T.; Mok, W. S. *Carbohydr. Res.* **1991**, *217*, 71–85.
38. Dias, A. S.; Lima, S.; Pillinger, M.; Valente, A. A. *Catal. Lett.* **2007**, *114*, 151–160.